

## Application of generalized differential quadrature method to nonlinear bending analysis of a single SWCNT over a bundle of nanotubes

A. FEREDOON<sup>1)</sup>, A. M. BABAEE<sup>2)</sup>, Y. ROSTAMIYAN<sup>1)</sup>

<sup>1)</sup>*Department of Mechanical Engineering  
Semnan University  
Semnan, P.O. Box 35195-363, Iran  
e-mails: ab.fereidoon@gmail.com,  
y.rostamiyan@iausari.ac.ir (corresponding author)*

<sup>2)</sup>*Department of Mechanical Engineering  
Islamic Azad University, Semnan Branch  
Semnan, P.O. Box 35145-179, Iran  
e-mail: a\_m\_babae@yahoo.com*

THE DEFORMATION OF AN INDIVIDUAL single walled carbon nanotube (SWCNT) over a bundle of nanotubes has been studied using the generalized differential quadrature (GDQ) method. The effects of length, diameter, and minimum value of Lennard–Jones experimental potential have been considered in the governing equation which is derived based on the GDQ and the issues related to the implementation of the boundary and compatibility conditions were addressed. The explanation of reliability and flexibility of the GDQ is done by solving several selected examples which are evaluated by comparing them with existing exact or approximate solutions which were previously generated by finite element approach.

**Key words:** generalized differential quadrature, SWCNT, bundle, bending.

Copyright © 2012 by IPPT PAN

### 1. Introduction

THE TUBULAR CARBON STRUCTURES were observed for the first time by IJIMA [1]. The nanotubes consisted of up to several tens of graphitic shells (so-called multi-walled carbon nanotubes (MWCNTs)) with adjacent shell separation of 0.34 nm, diameters of 1 nm and large length/diameter ratio. Later, IJIMA and ICHIHASHI [2] and BETHUNE *et al.* [3] synthesized single-walled carbon nanotubes (SWCNTs). The synthesized nanotube samples are characterized by means of Raman, electronic, and optical spectroscopies. Important information is derived by mechanical, electrical and thermal measurements. Along with the improvement of the production and characterization techniques for nanotubes, progress is being made in their application. The estimated high Young's modulus and tensile strength of the nanotubes led to speculations for their pos-

sible use in composite materials with improved mechanical properties [4] and actually resulted in production of new materials [5–7].

The configuration of the current problem consists of a single SWCNT over a bundle of nanotubes which is assumed to be rigid due to relative mechanical properties. The van der Waals interaction plays an important role on the performance of SWCNT structures, such as mechanical properties [8–11]. The van der Waals nonlinear interaction plays the most important role in the variation of separation distance between individual SWCNT and its substrate. WONG *et al.* [12] employed a cantilevered beam model in their research in which a microscopic point force bent a single MWCNT. SALVETAT *et al.* [9, 13] used the simply-supported beam model to simulate the deflections of the MWCNTs and of some different kinds of SWCNT ropes. In the current study the effects of physical SWCNT properties on the deflection of an individual SWCNT in different substrate curvature are investigated by modelling the SWCNT as an Euler–Bernoulli beam model. Generalized differential quadrature (GDQ) is implemented as a practical numerical method in solving higher order differential equation [15–17], to solve the governing equation of nanotube as a beam model. The proposed GDQ employs the same number of independent variables as that of the conditions at any discrete point. Therefore, the GDQ can deal with the differential equations, which may be constrained by multiple conditions at any discrete point. Several recent publications have reviewed the modelling and simulation of carbon nanotubes and nanocomposites mechanical properties [18–20]. But these review articles do not cover separation of an individual SWCNT from a substrate of its own kind. Therefore the purpose of this study is the explanation of reliability and flexibility of the GDQ by solving several selected examples which are evaluated by comparing them with the existing exact or approximate solutions that were previously generated by finite element approach.

## 2. Formulations

### 2.1. Schematic of problem

As shown in Fig. 1 the problem configuration consist of two main parts, one is an individual SWCNT and the other is a bundle of nanotubes which plays a role as a substrate. To fix a situation of coordinate axis the substrate curvature is assumed to be a parabolic which is shown in Fig. 1.

The analytical equation of the above mentioned parabolic substrate which curvature constant is  $m$ , will be:

$$(2.1) \quad y = \frac{m}{2}x^2.$$

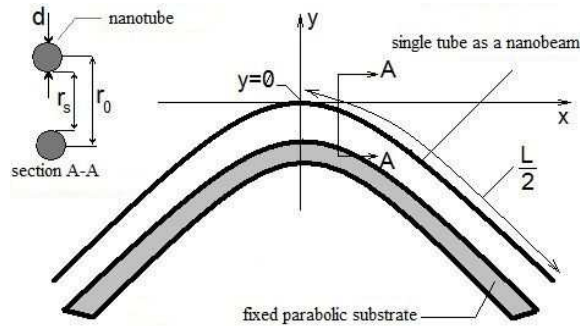


FIG. 1. Initial condition of the nanobeam model.

From KUDIN [21] the stiffness of the nanotube and its diameter have the following relationship:

$$(2.2) \quad EI = \pi C d^3,$$

where  $EI$  is the bending stiffness and  $C$  is  $2152.8 \text{ eV/nm}^2$  which is computed for in-plane stiffness based on ab initio calculations, and  $d$  is the diameter of the tube. From Fig. 2 it is easily recognized that bending stiffness of the bundle is much bigger than the individual SWCNT [22]. This means that assuming the substrate as a rigid body will be acceptable.

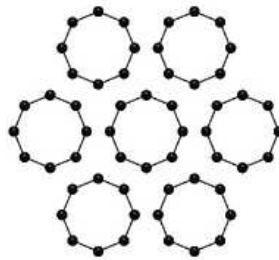


FIG. 2. Schematic of a bundle of nanotubes consist of 7 SWCNTs, [22].

In Fig. 2, the diameter of the bundle is about 4 times bigger than each individual SWCNT diameter [22] thus its bending stiffness is  $4^3$  times bigger than for each individual SWCNT (Eq. 2.2).

## 2.2. Modeling the individual SWCNT as a beam

Based on aspect ratio of SWCNTs and their mechanical properties, the simulation of SWCNT as a straight inextensible beam is acceptable [14, 23, 24], the only interaction force between nanotubes is the van der Waals force [18–24] which is determined in many papers from experimental Lennard–Jones potential [24–26]. Using the above information and the Euler beam theory for single

SWCNT will determine the governing equation which explains the deflection of the individual tube.

From the Euler beam theory the governing equation of the one-dimensional inextensible beam is [27, 28]:

$$(2.3) \quad \frac{d^2}{dX^2} \left( EI \frac{d^2 y}{dX^2} \right) + F_{\text{substrate}} = -F_{\text{external}}.$$

Figure 1 shows the symmetry of the  $y$  axis; therefore, the analysis of a one-half of SWCNT is sufficient to obtain the results. The only force that acts is van der Waals force which is expressed in per unit length as [25]:

$$(2.4) \quad F(r(X)) = 17.81U_0 \left[ - \left( \frac{3.41}{3.13 \frac{r(X)+r_0-d}{r_0-d} + 0.28} \right)^{11} + \left( \frac{3.41}{3.13 \frac{r(X)+r_0-d}{r_0-d} + 0.28} \right)^5 \right],$$

where  $U_0$  is the minimum energy in the Lennard–Jones energy potential,  $r_s$  is the distance between the surfaces of nanobeam and substrate when the van der Waals force is zero (Fig. 1),  $r_0$  is the distance which is measured by  $r_0 = r_s + d$  where  $d$  is the diameter of the nanobeam and  $r(X)$  is an offset distance between the surfaces of nanobeam and substrate during deformation. From Eq. (2.1) the curvature of an individual SWCNT has the following form:

$$(2.5) \quad y(X) = \frac{m}{2} X^2 + r(X).$$

The boundary conditions due to symmetry and configuration of the problem will be:

$$(2.6) \quad \begin{aligned} y^{(1)}(0) &= 0, & y^{(3)}(0) &= 0, \\ y^{(2)}(L) &= 0, & y^{(3)}(L) &= 0. \end{aligned}$$

Considering Eq. (2.5), the governing equation and the boundary conditions in Eq. (2.5) will be:

$$(2.7) \quad EI \frac{d^4 r(X)}{dX^4} + F(r(X)) = 0,$$

with boundary conditions

$$(2.8) \quad \begin{aligned} r^{(1)}(0) &= 0, & r^{(3)}(0) &= 0, \\ r^{(2)}(L) &= -m, & r^{(3)}(L) &= 0. \end{aligned}$$

By applying the Taylor series expansion to the van der Waals force and truncating higher order terms one can simplify high order nonlinearities to practical form as follows:

$$(2.9) \quad F_{\text{van der Waals}} \approx -1.10^{-8} + 274.5242066r(X) + O(r^2(X)).$$

### 2.3. Differential quadrature and solution procedure

The GDQ method has been proved to be an efficient higher-order numerical technique for the solution of initial and boundary value problems. The GDQ technique has been widely reported to yield successful solutions for various dynamic and stability problems [29–36]. The essence of the GDQ method is that a derivative of a function  $F$  is approximated as a weighted linear sum of all functional values within the computational domain

$$(2.10) \quad \left. \frac{d^n F}{dX^n} \right|_{X=X_i} = \sum_{j=1}^N c_{ij}^n F(X_j),$$

where

$$(2.11) \quad c_{ij}^1 = \frac{\pi(X_j)}{(X_i - X_j)(\pi(X_i))}; \quad i, j = 1, 2, \dots, N, \quad i \neq j,$$

where  $\pi(X_i)$  is defined as:

$$(2.12) \quad \pi(X_i) = \prod_{j=1, j \neq i}^N (X_i - X_j), \quad i \neq j.$$

When  $i = j$ :

$$(2.13) \quad c_{ii}^1 = c_{ii}^1 = - \sum_{k=1, k \neq i}^N c_{ik}^1, \quad i = 1, 2, \dots, N, \quad i \neq k, \quad i = j,$$

where  $N$  is the number of grid points along the  $x$  direction. The weighting coefficients for the second, third and fourth derivatives are determined by the following formula:

$$(2.14) \quad c_{ij}^{(m)} = m \left( c_{ij}^1 c_{ii}^{(m-1)} - \frac{c_{ij}^{(m-1)}}{(X_j - X_i)} \right),$$

$$i, j = 1, 2, \dots, N, \quad i \neq j, \quad m = 2, 3, \dots, N - 1,$$

$$(2.15) \quad c_{ii}^{(m)} = - \sum_{j=1, j \neq i}^N c_{ij}^{(m)}, \quad i = 1, 2, \dots, N, \quad i \neq k, \quad i = j.$$

One of the most accurate meshes in GDQ formulation are Chebyshev nodes which are defined by following inverse node numbering:

$$(2.16) \quad X_i = X_1 + \frac{1}{2} \left( 1 - \cos \frac{i-1}{N-1} \pi \right) (X_N - X_1), \quad i = 1, 2, \dots, N.$$

For convenience and generality the following nondimensional variables are introduced in the present analysis:

$$(2.17) \quad x = \frac{X}{L},$$

where  $x$  is nondimensional variable which varies between 0 to 1,  $L$  is the length of nanotube and  $X$  represents vertical axis before nondimensionalisation. By this assumption the derivatives will have the following form:

$$(2.18) \quad \begin{aligned} \frac{dr}{dX} &= \frac{dr}{Ldx}, \\ \frac{d^3r}{dX^3} &= \frac{1}{L^3} \frac{d^3r}{dx^3}, \\ \frac{d^4r}{dX^4} &= \frac{1}{L^4} \frac{d^4r}{dx^4}. \end{aligned}$$

After nondimensionalisation the governing equation will be:

$$(2.19) \quad EI \frac{1}{L^4} \frac{d^4r(x)}{dx^4} + F(r(x)) = 0$$

with boundary conditions

$$(2.20) \quad r^{(1)}(0) = 0, \quad r^{(3)}(0) = 0, \quad r^{(2)}(1) = -mL^2, \quad r^{(3)}(1) = 0.$$

By applying Eqs. (2.10)–(2.20)

$$(2.21) \quad \frac{EI}{L^4} \begin{bmatrix} c_{11}^{(4)} & c_{12}^{(4)} & \dots & c_{1(n-1)}^{(4)} & c_{1n}^{(4)} \\ c_{21}^{(4)} & c_{22}^{(4)} & & c_{2(n-1)}^{(4)} & c_{2n}^{(4)} \\ \cdot & & & & \cdot \\ \cdot & & & & \cdot \\ \cdot & & & & \cdot \\ c_{(n-1)1}^{(4)} & c_{(n-1)2}^{(4)} & & c_{(n-1)(n-1)}^{(4)} & c_{(n-1)n}^{(4)} \\ c_{n1}^{(4)} & c_{n2}^{(4)} & \dots & c_{n(n-1)}^{(4)} & c_{nn}^{(4)} \end{bmatrix} \begin{bmatrix} r_1 \\ r_2 \\ \cdot \\ \cdot \\ \cdot \\ r_{(n-1)} \\ r_n \end{bmatrix} + \begin{bmatrix} 274.5242066r_1 \\ 274.5242066r_2 \\ \cdot \\ \cdot \\ \cdot \\ 274.5242066r_{(n-1)} \\ 274.5242066r_n \end{bmatrix} = \begin{bmatrix} 1.10^{-8} \\ 1.10^{-8} \\ \cdot \\ \cdot \\ \cdot \\ 1.10^{-8} \\ 1.10^{-8} \end{bmatrix}.$$

Because of high instability on borders, for applying boundary conditions, the above equations should be substituted into first, second,  $(n - 1)$ -th and last line of Eq. (2.21):

$$(2.22) \quad \begin{bmatrix} c_{11}^{(1)} & c_{12}^{(2)} & \dots & c_{1(n-1)}^{(1)} & c_{1n}^{(1)} \\ c_{11}^{(3)} y & c_{12}^{(3)} & \dots & c_{1(n-1)}^{(3)} & c_{1n}^{(3)} \\ \frac{EI}{L^4} c_{31}^{(4)} & \frac{EI}{L^4} c_{41}^{(4)} & \dots & \frac{EI}{L^4} c_{32}^{(4)} & \frac{EI}{L^4} c_{42}^{(4)} \\ \frac{EI}{L^4} c_{3(n-1)}^{(4)} & \frac{EI}{L^4} c_{4(n-1)}^{(4)} & \dots & \frac{EI}{L^4} c_{3n}^{(4)} & \frac{EI}{L^4} c_{4n}^{(4)} \\ \cdot & \cdot & \dots & \cdot & \cdot \\ \cdot & \cdot & \dots & \cdot & \cdot \\ \cdot & \cdot & \dots & \cdot & \cdot \\ \frac{EI}{L^4} c_{(n-3)1}^{(4)} & \frac{EI}{L^4} c_{(n-3)2}^{(4)} & \dots & \frac{EI}{L^4} c_{(n-3)(n-1)}^{(4)} & \frac{EI}{L^4} c_{(n-3)n}^{(4)} \\ \frac{EI}{L^4} c_{(n-2)1}^{(4)} & \frac{EI}{L^4} c_{(n-2)2}^{(4)} & \dots & \frac{EI}{L^4} c_{(n-2)(n-1)}^{(4)} & \frac{EI}{L^4} c_{(n-2)n}^{(4)} \\ c_{n1}^{(2)} & c_{n2}^{(2)} & \dots & c_{n(n-1)}^{(2)} & c_{nn}^{(2)} \\ c_{n1}^{(3)} & c_{n2}^{(3)} & \dots & c_{n(n-1)}^{(3)} & c_{nn}^{(3)} \end{bmatrix} \begin{bmatrix} r_1 \\ r_2 \\ \cdot \\ \cdot \\ \cdot \\ r_{(n-1)} \\ r_n \end{bmatrix} + \begin{bmatrix} 0 \\ 0 \\ 274.5242066 r_3 \\ 274.5242066 r_4 \\ \cdot \\ \cdot \\ \cdot \\ 274.5242066 r_{(n-3)} \\ 274.5242066 r_{(n-2)} \\ mL^2 \\ 0 \end{bmatrix} = \begin{bmatrix} 0 \\ 0 \\ 1.10^{-8} \\ \cdot \\ \cdot \\ \cdot \\ 1.10^{-8} \\ 0 \\ 0 \end{bmatrix} .$$

Clearly, the above set of equations can be solved using several known methods.

**2.4. Finite element method (FEM)**

FEM is applied to the governing equation in order to do verification, and corresponding results show the great agreement between analytical and FEM

solutions. Expressing Eq. (2) in the Galerkin weak form:

$$(2.23) \quad \int_{x=0}^L \left( EI \frac{d^2 w(x)}{dx^2} \frac{d^2 r}{dx^2} + w(x) F(r(x)) \right) dx = -mEI \frac{dw(x)}{dx} \Big|_{x=L},$$

where  $w(x)$  is acceptable test function. In terms of force, using the Newton–Raphson method, yields:

$$(2.24) \quad F(r) = F(\bar{r}_0) + \frac{d}{dr} F(\bar{r}_0) \Delta r + O(\Delta r^2),$$

$w$  is assumed to be:

$$(2.25) \quad w = \sum_{A \in \eta_g} C_A \Phi_A,$$

and  $\Delta r$  will be determined by:

$$(2.26) \quad r = \sum_{B \in \eta} (d_B + \Delta d_B) \Phi_B,$$

$$(2.27) \quad \Delta r = \sum_{B \in \eta} \Delta d_B \Phi_B,$$

where  $\Phi$  is shape function, computed values of  $d_B$  are used to evaluate the  $\Delta d_B$  which is an unknown variable, the set of all unknown degrees of freedom at points grid in the FEM mesh is  $\eta_g$  and the total number of points grid multiplied by the degrees of freedom at each point is called  $\eta$ . Equation (2.24) is substituted into Eq. (2.23) and then the Newton–Raphson approach is applied to derive Eq. (2.28):

$$(2.28) \quad \sum_{A \in \eta_g} C_A \left[ \sum_{B \in \eta} \left( \int_{x=0}^L EI \frac{d^2 \Phi_A}{dx^2} \frac{d^2 \Phi_B}{dx^2} dx + \int_{x=0}^L \Phi_A \frac{dF(\bar{r}_0)}{dr} \Phi_B dx \right) \Delta d_B \right] =$$

$$-mEI \frac{dw(x)}{dx} \Big|_{x=L} - \sum_{A \in \eta_g} C_A \left[ \int_{x=0}^L \Phi_A F(\bar{r}_0) dx + \sum_{B \in \eta_g} \left( \int_{x=0}^L EI \frac{d^2 \Phi_A}{dx^2} \frac{d^2 \Phi_B}{dx^2} dx \right) d_B \right]$$

explaining

$$\begin{aligned}
 K_{AB} &= \int_{x=0}^L EI \frac{d^2\Phi_A}{dx^2} \frac{d^2\Phi_B}{dx^2} dx, \\
 K_{AB}^* &= \int_{x=L}^L \Phi_A \frac{dF(\bar{r}_0)}{dr} \Phi_B dx, \\
 F_A &= \int_{x=0}^L \Phi_A F(\bar{r}_0) dx,
 \end{aligned}
 \tag{2.29}$$

and rewriting Eq. (2.28):

$$\begin{aligned}
 \sum_{A \in \eta_g} C_A \left[ \sum_{B \in \eta} (K_{AB} + K_{AB}^*) \Delta d_B \right] \\
 = -mEI \frac{dw(x)}{dx} \Big|_{x=L} - \sum_{A \in \eta} C_A \left[ \sum_{B \in \eta} K_{AB} d_B + F_A \right].
 \end{aligned}
 \tag{2.30}$$

Hermite interpolation polynomials which are used should be at least of order 3, because every element has four unknowns.

$$\begin{aligned}
 \Phi_1^e(x) &= 1 - 3s^2 + 2s^3, \\
 \Phi_2^e(x) &= l^e s(s - 1)^2, \\
 \Phi_3^e(x) &= s^2(3 - 2s), \\
 \Phi_4^e(x) &= l^e s^2(s - 1),
 \end{aligned}
 \tag{2.31}$$

$l^e$  represents the length of one element,  $s$  is determined by  $(x - x_1)/(x_2 - x_1)$ , where  $x_1$  and  $x_2$  are the left and right values of coordinates axis of the element. The first step to assess a value for  $d_B$  is important for converging the Newton–Raphson approach. Because Eq. (2.30) is highly nonlinear equation, an incremental load is used. At the beginning the curvature of the substrate is assumed to be zero and resultant solutions are taken as initial guess. In the next step the larger curvature of substrate is used, for the initial guess in this step the solution of the previous step is used therefore the convergence of the approach is determined. The above steps are repeated until a required  $m$  is reached.

### 3. Results

#### 3.1. Mesh point number effect

Because of the high importance of the number of points required in the grid to converge the approach, it should be examined. As a simple illustration, Figs. 3 and 4 use 100 point grids and continuity of results is visible. Deformation behavior and interaction force are depicted in Figs. 3 and 4, respectively.

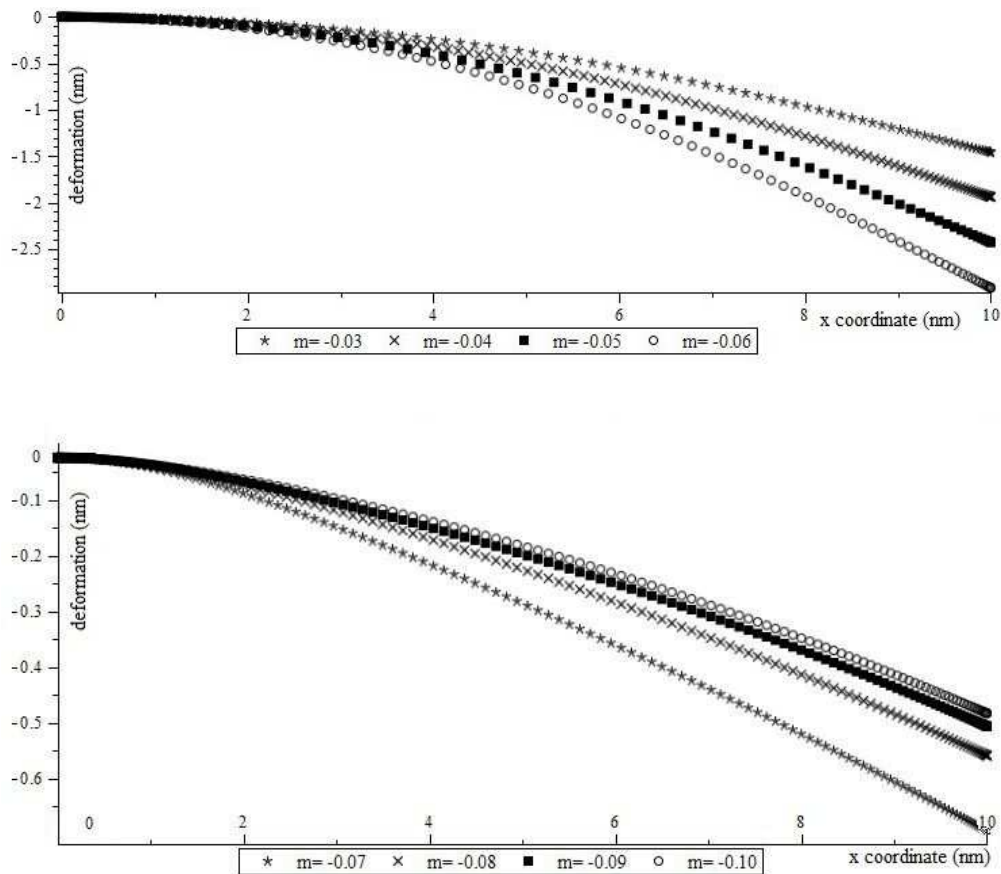


FIG. 3. Deformation of single SWCNT ( $2L = 20$ ,  $d = 0.4$ ) and the mesh grid has 100 points.

By substituting the deformation results into Eq. (2.4), the van der Waals interaction will be shown in Fig. 4, which has an adequate accuracy from the engineering point of view.

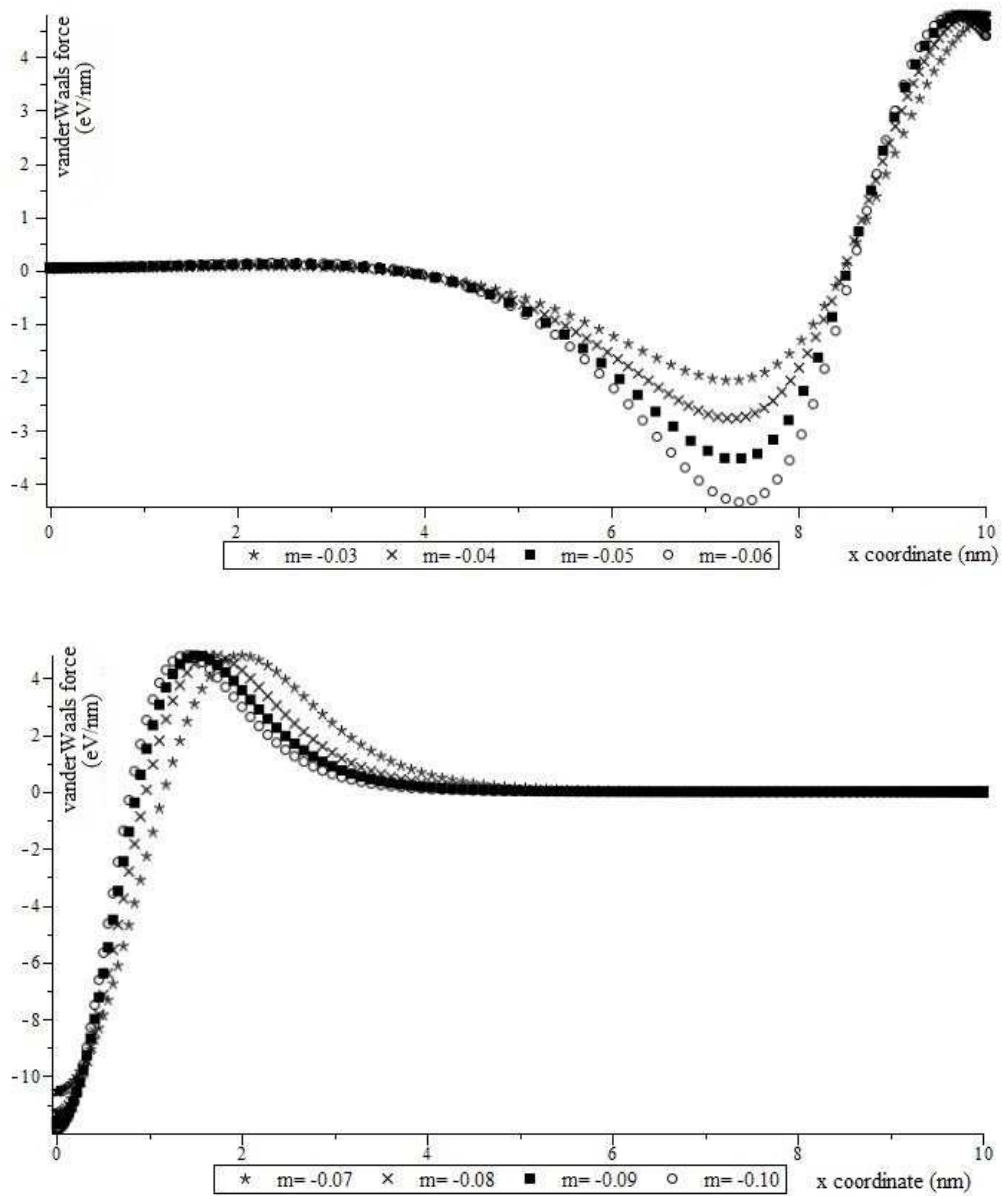


FIG. 4. Interacting force of single SWCNT ( $2L = 20$ ,  $d = 0.4$ ) and the mesh grid has 100 points.

Figure 5 shows the results for the same SWCNT which uses 20 points. The deformation response results emphasize the instability in this approach resulting from the mesh grid.

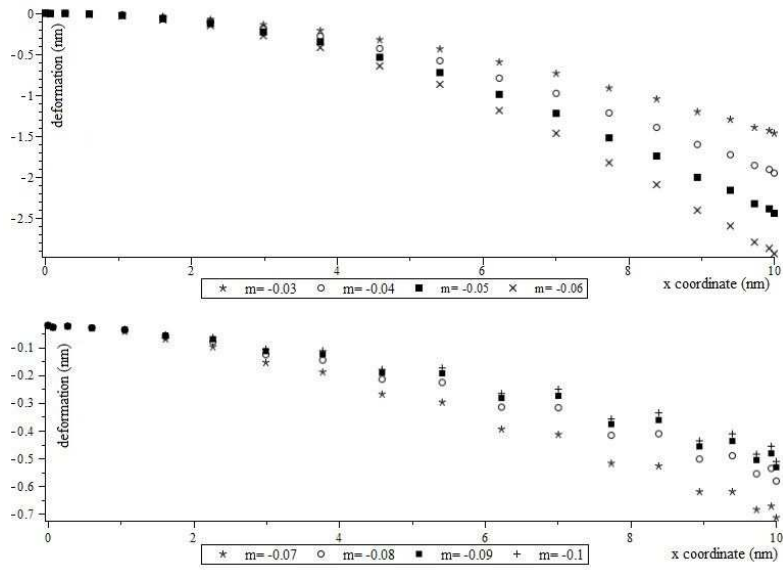


FIG. 5. Deformation of single SWCNT ( $2L = 20$ ,  $d = 0.4$ ) and the mesh grid has 20 points.

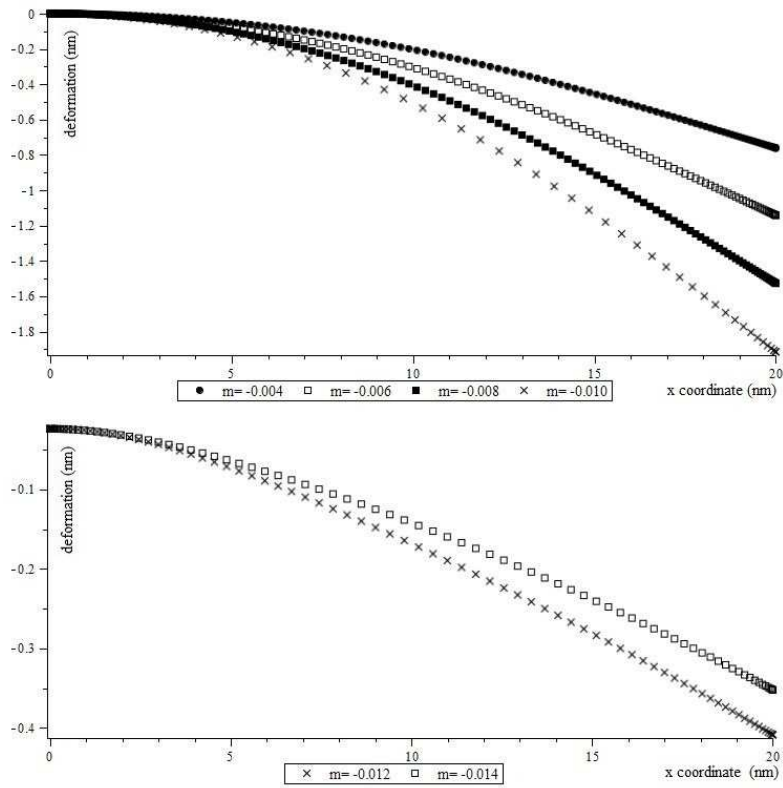


FIG. 6. Deformation of single SWCNT ( $2L = 40$ ,  $d = 1.4$ ) and the mesh grid has 100 points.

### 3.2. Length effect

Herein the length of SWCNT is the parameter which is studied in GDQ results and each case is solved for 100 points grid. In Figs. 6 and 7 the length of the individual SWCNT is  $2L = 40$  nm and the diameter is 1.4 nm and these figures are about deformation and interaction, respectively. The observed behaviors are similar to those which were seen in Fig. 3.

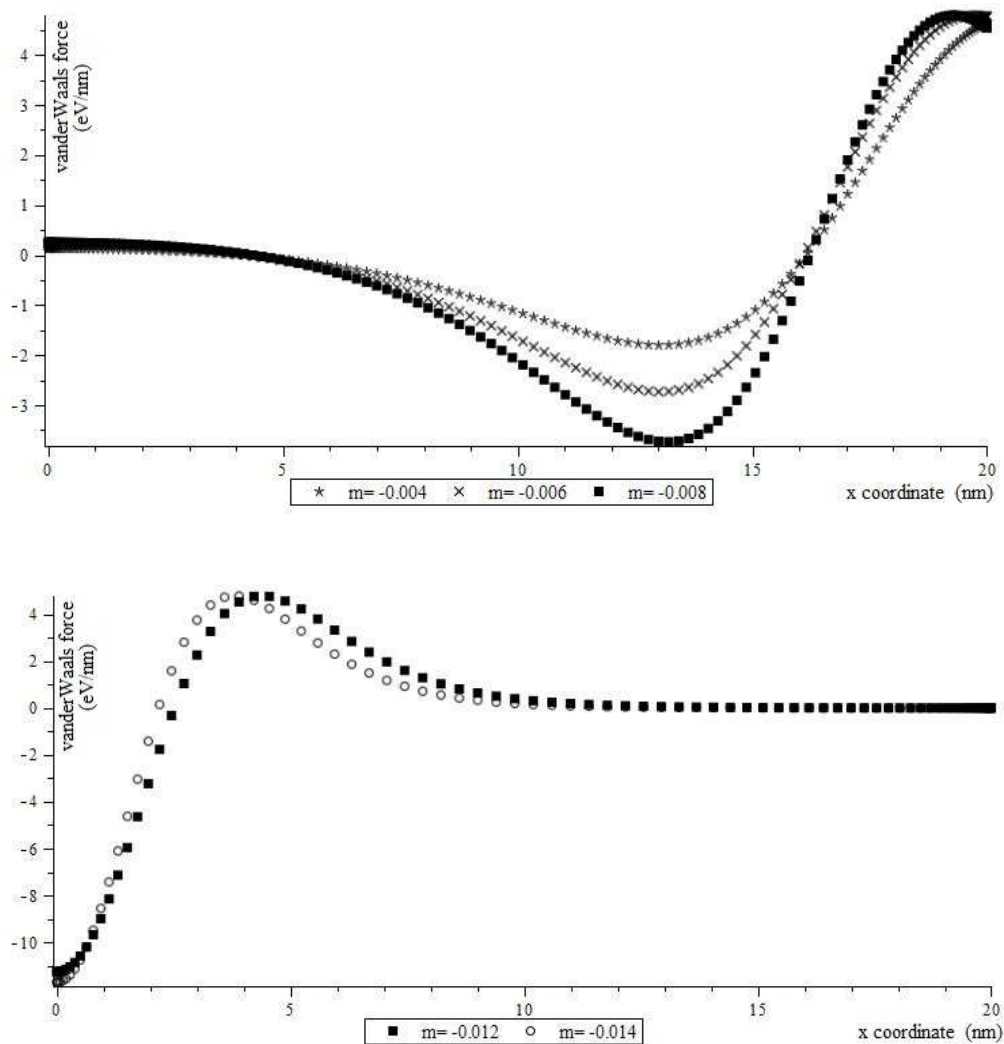


FIG. 7. Interacting force of single SWCNT ( $2L = 40$ ,  $d = 1.4$ ) and the mesh grid has 100 points.

Using last results and Eq. (2.4), the interactions in the above case are plotted in Fig. 7 again reasonable values are obtained.

Figures 7 and 8 show the results related to SWCNT which has the length of 200 nm and the diameter of 1.4 nm. Figure 8 is related to deformation manner.

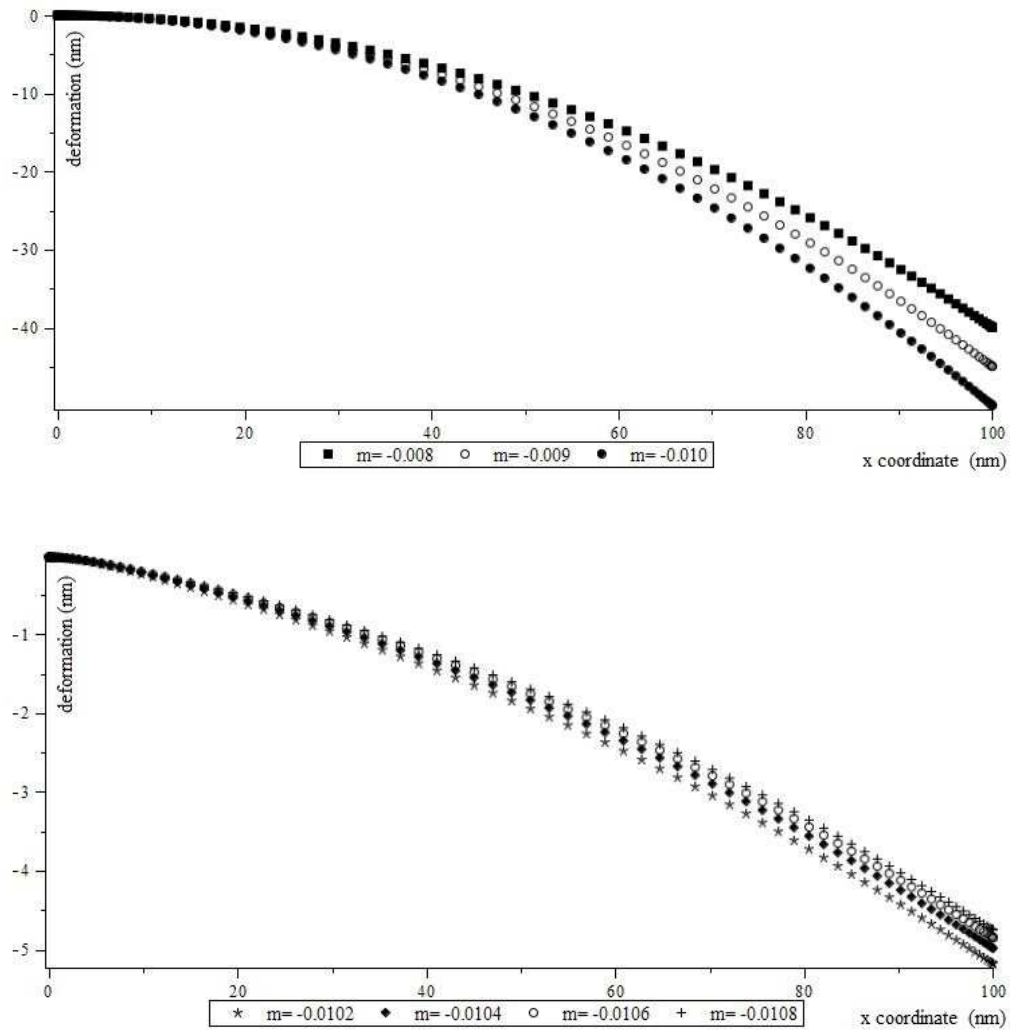


FIG. 8. Deformation of single SWCNT ( $2L = 200$ ,  $d = 1.4$ ) and the mesh grid has 100 points.

After obtaining deformation values, interaction will be achieved by Eq. (2.4), the related responses are displayed in Fig. 9.

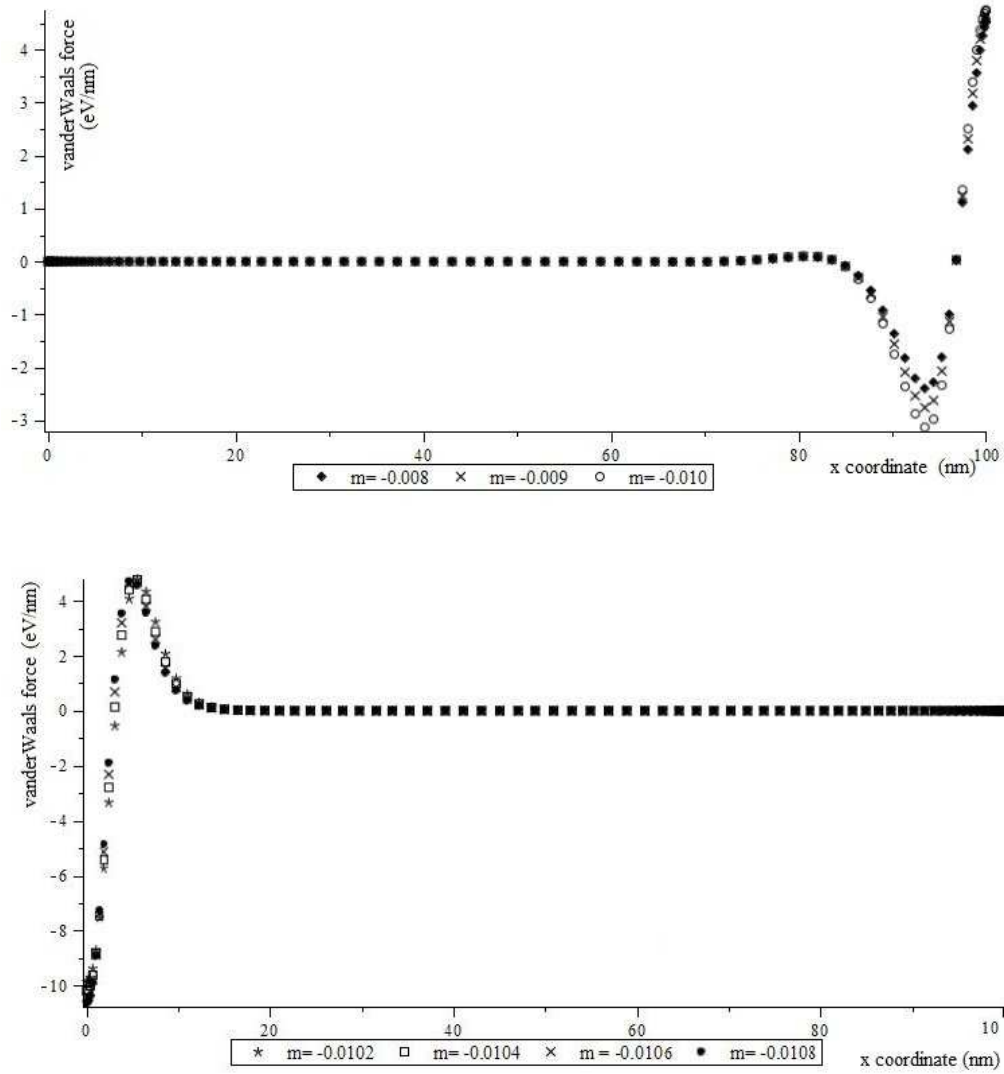
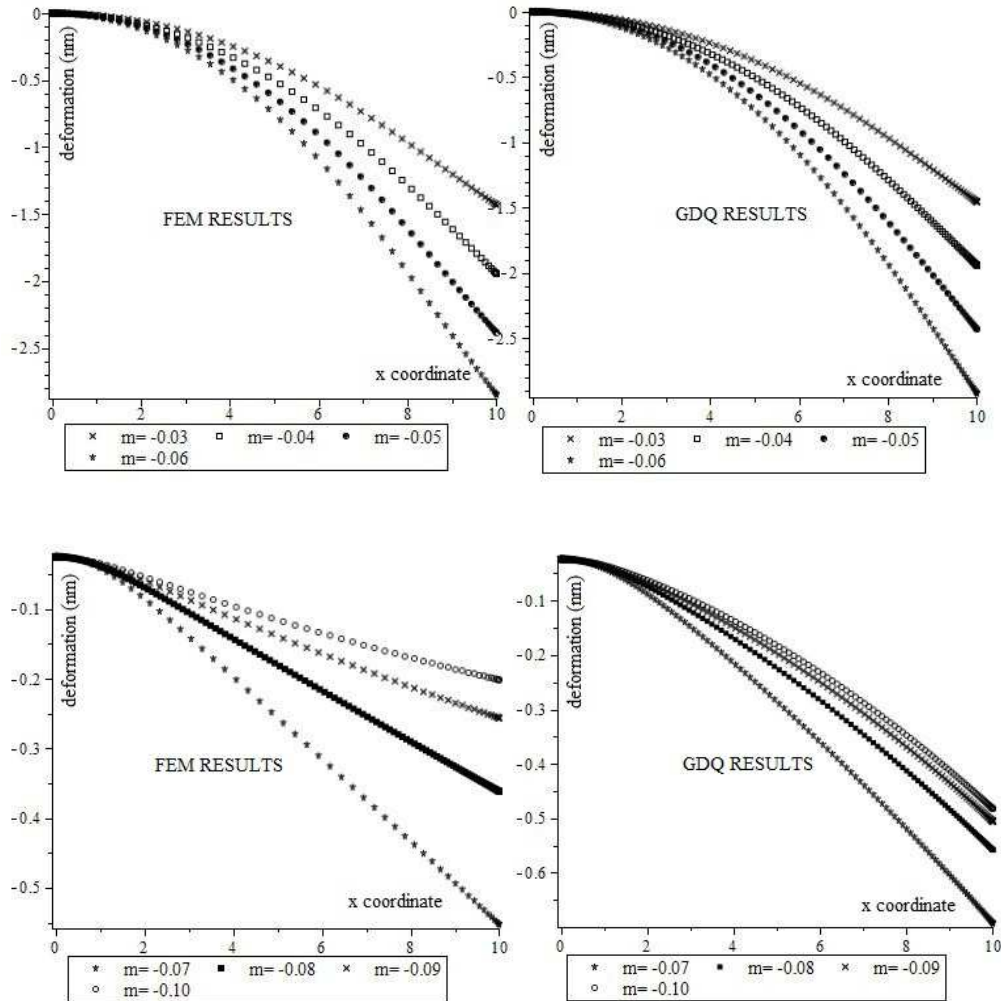


FIG. 9. Interacting force of single SWCNT ( $2L = 200$ ,  $d = 1.4$ ) and the mesh grid has 100 points.

### 3.3. Validation of GDQ approach

To validate the present GDQ approach for deformation solutions of the SWCNT, comparisons have been carried out with the results of LI *et al.* [24]. In their analysis, finite element method was used to describe the deformation of the individual nanotube.

The research was performed in two cases, the first one belongs to a single tube which has the length of 20 nm and the diameter of 1.4 nm. Corresponding responses are depicted in Fig. 10.

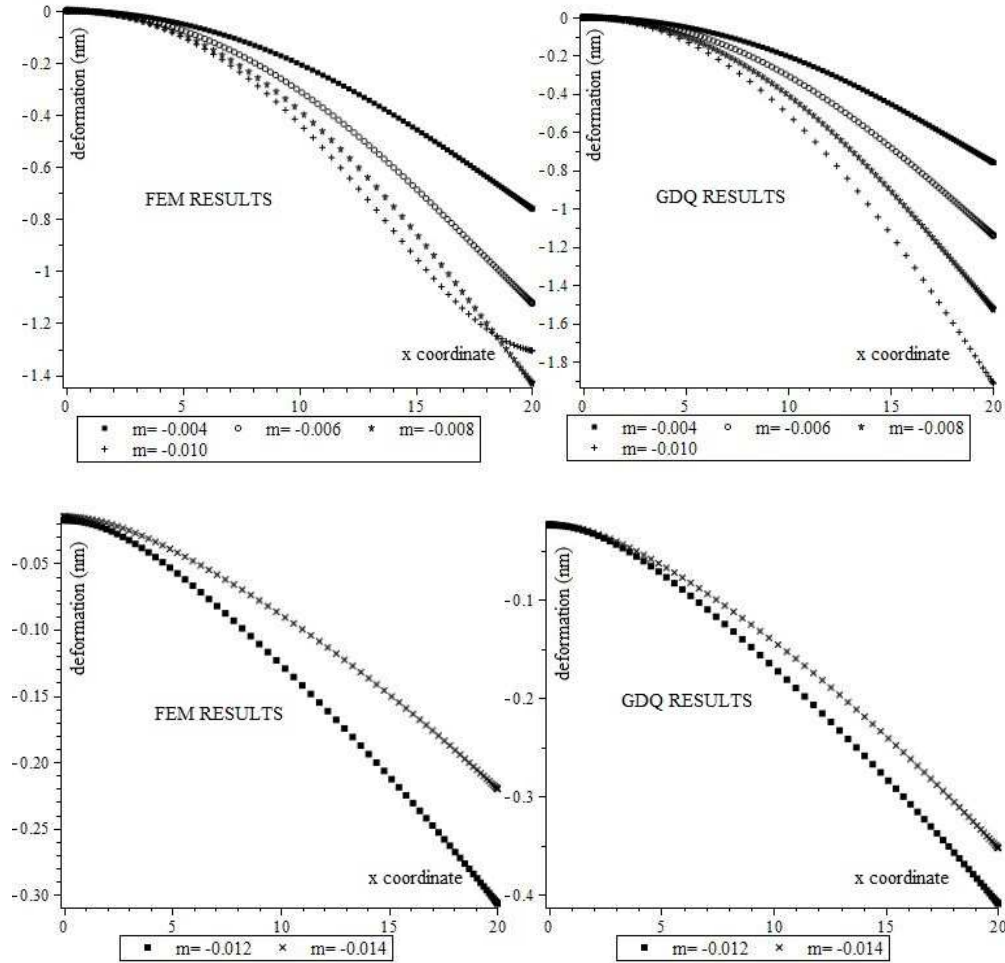


1. FEM method's results, [24].

2. GDQ method's results.

FIG. 10. Deformation of single SWCNT ( $2L = 20$ ,  $d = 0.4$ ) and the mesh grid has 100 points.

In the second case, the nanotube has the length of 40 nm and the diameter of 1.4 nm. Computations related to this case are depicted in Fig. 11.



1. FEM method's results, [24].

2. GDQ method's results.

FIG. 11. Deformation of single SWCNT ( $2L = 40$ ,  $d = 1.4$ ) and the mesh grid has 100 points.

#### 4. Conclusion

The deformation of individual SWCNT located over a bundle of nanotube is analyzed based on small deformation theory and the Euler beam theory. The van der Waals forces are significant in SWCNTs which are located closely. Influence of the length and diameter of the individual SWCNT beside the curvature of substrate on deformation behavior of the single SWCNTs is shown. The governing equation and the boundary conditions for the SWCNT as an Euler beam

are solved using the GDQ method. From the GDQ solutions, it can be clearly seen that the length of a single SWCNT has a great effect of deformation behavior related to the same curvature. With the same SWCNT the number of mesh points is important especially in distribution of interacting forces. As a parameter the aspect ratio is important and it is obvious that in small aspect ratio the individual SWCNT can deform more significantly and be near the substrate in high curvature value of substrate.

Validations of the present GDQ approach have been carried out by comparisons with the results of LI *et al.* [24]. In their analysis, finite element method was used to describe the deformation of the individual nanotube. The comparisons illustrate the stability and continuity of results of GDQ method beside rapid convergence in this method.

## References

1. S. IJIMA, *Helical microtubules of graphitic carbon*, Nature (London), **354**, 56–58, 1991.
2. S. IJIMA, T. ICHIHASHI, *Single-shell carbon nanotubes of 1 nm diameter*, Nature (London), **356**, 776–778, 1993.
3. D.S. BETHUNE, C.H. KIANG, M.S. DE VRIES, G. GORMAN, R. SAVOY, J. VAZQUEZ, R. BEYERS, *Cobalt-catalysed growth of carbon nanotubes with single-atomic-layer walls*, Nature (London), **363**, 605–607, 1993.
4. G. OVERNEY, W. ZHONG, D. TOMÁNEK, *Structural rigidity and low frequency vibrational modes of long carbon tubules*, Phys. D, **27**, 93–96, 1993.
5. S.P.M. SHAFFER AND J.K.W. SANDLER, *Carbon Nanotube/Nanofibre Polymer Composites*, Chapter 1, [in:] Processing and Properties of Nanocomposites, World Scientific Publishing Co. Pte. Ltd. <http://www.worldscibooks.com/nanosci/6317.html>.
6. LI XU, CONG YUE, J. LIU, Y. ZHANG, X. Z. LU, Z. CHENG, *Nano-thermal interface material with CNT nano-particles for heat dissipation application*, International Conference on Electronic Packaging Technology & High Density Packaging (ICEPT-HDP), p. 4, 2008.
7. X. GUO, T. ZHANG, *A study on the bending stiffness of single-walled carbon nanotubes and related issues*, Journal of the Mechanics and Physics of Solids, **58**, 428–443, 2010.
8. E. SAETHER, S.J.V. FRANKLAND, R.B. PIPES, *Transverse mechanical properties of single-walled carbon nanotube crystals, Part I: Determination of elastic moduli*, Compos. Sci. Technol., **63**, 1543–1550, 2003.
9. J.P. SALVETAT, G.A.D. BRIGGS, J.M. BONARD, R.R. BACSA, A.J. KULIK, T. STOCKLI, N.A. BURNHAM, L. FORRO, *Elastic and shear moduli of single-walled carbon nanotube ropes*, Phys. Rev. Lett., **82**, 944–947, 1999.
10. A. FEREIDON, N. KORDANI, A. GHORBANZADEH AHANGARI, M. ASHOORY, *Damping augmentation of epoxy using carbon nanotubes* Int. J. Polym. Mater., **60**, 11–26, 2011.
11. A. KRISHNAN, E. DUJARDIN, T.W. EBBESEN, P.N. YIANILOS, M.M.J. TREACY, *Young's modulus of single-walled nanotubes*, Phys. Rev. B., **58**, 14013–14019, 1998.

12. E.W. WONG, P.E. SHEEHAN, C.M. LIEBER, *Nanobeam mechanics: elasticity, strength, and toughness of nanorods and nanotubes*, Science, **277**, 1971–1975, 1997.
13. J.P. SALVETAT, A.J. KULIK, J.M. BONARD, G.A.D. BRIGGS, T. STOCKLI, K. METENIER, S. BONNAMY, F. BEGUIN, N.A. BURNHAM, L. FORRO, *Elastic modulus of ordered and disordered multiwalled carbon nanotubes*, Adv. Mater., **11**, 161–165, 1999.
14. D.H. ROBERTSON, D.W. BRENNER, J.W. MINTMIRE, *Energetics of nanoscale graphitic tubules*, Phys. Rev. B., **45**, 12592–12595, 1992.
15. T.Y. WU, G.R. LIU, *The differential quadrature as a numerical method to solve the differential equation*, Comput. Mech., **24**, 197–205, 1999.
16. T.Y. WU, G.R. LIU, *A generalized differential quadrature rule for initial-value differential equations*, J. Sound Vib., **233**, 195–213, 2000.
17. G.R. LIU, T.Y. WU, *Numerical solution for differential equations of Duffng-type nonlinearity using the generalized differential quadrature rule*, J. Sound Vib., **237**, 805–817, 2000.
18. Z. SPITALSKYA, D. TASISB, K. PAPAGELISB, C. GALIOTIS, *Carbon nanotube–polymer composites: Chemistry, processing, mechanical and electrical properties*, Progress in Polymer Science, **35**, 357–401, 2010.
19. V.N. POPOV, *Carbon nanotubes: properties and application*, Materials Science and Engineering R., **43**, 61–102, 2004.
20. M. SAMMALKORPI, A.V. KRASHENINNIKOV, A. KURONEN, K. NORDLUND, B.K. KASKI, *Irradiation-induced stiffening of carbon nanotube bundles*, Nuclear Instruments and Methods in Physics Research B., **228**, 142–145, 2005.
21. K.N. KUDIN, G.E. SCUSERIA, B.I. YAKOBSON, *C<sub>2</sub>F, BN, and C nanoshell elasticity from ab initio computations*, Physical Review B, **64**. 235406-10, 2010.
22. D. QIAN, W.K. LIU, R.S. RUOFF, *Load transfer mechanism in carbon nanotube ropes*, Composites Sci. Techn., **63**, 1561–1569, 2003.
23. R.F. GIBSON, E.O. AYORINDE, Y.F. WEN, *Vibrations of carbon nanotubes and their composites: A review*, Composites Science and Technology, **67**, 1–28, 2007.
24. Z. LI, P. DHARAP, S. NAGARAJAIAH, R.P. NORDGREN, B. YAKOBSON, *Nonlinear analysis of a SWCNT over a bundle of nanotubes*, International Journal of Solids and Structures, **41**, 6925–6936, 2004.
25. J.N. ISRAELACHVILI, *Intermolecular and Surface Forces*, 2nd ed., Academic Press, Harcourt Brace & Company Publishers, 1991.
26. D.W. COFFIN, L.A. CARLSSON, R.B. PIPES, *On the separation of carbon nanotubes*, Composites Science and Technology, **66**, 1132–1140, 2006.
27. M. HETENYI, *Beams on Elastic Foundation*, Ann Arbor the University of Michigan Press, London 1946.
28. A.P. BORESI, R.J. SCHMIDT, *Advanced Mechanics of Materials*, 6th ed., Wiley, 1954.
29. R. BELLMAN, B.G. KASHEF, J. CASTI, *A technique for the rapid solution of nonlinear partial differential equations*, Comput. Phys., **10**, 40–52, 1972.
30. F. CIVAN, C.M. SLIEPCEVICH, *Application of differential quadrature to solution of pool boiling in cavities*, Comput. Phys., **56**, 343–348, 1984.

31. C.W. BERT, S.K. JANG, A.G. STRIZ, *Nonlinear bending analysis of orthotropic rectangular plates by the method of differential quadrature*, AIAA. J., **26**, 612–618, 1988.
32. S.K. JANG, C.W. BERT, A.G. STRIZ, *Application of differential quadrature to static analysis of structural components*, Int. J. Num. Methods Eng., **28**, 561–577, 1989.
33. A.N. SHERBOURNE, M.D. PANDEY, *Differential quadrature method in the buckling analysis of beams and composite plates*, Comput. Struct., **40**, 903–913, 1990.
34. R.H. MOHAMMAD, J.A. MOHAMMAD, P. MALEKZADEH, *A differential quadrature analysis of unsteady open channel flow*, Appl. Math. Modelling, **31**, 1594–1608, 2007.
35. S.C. PRADHAN, T. MURMU, *Thermo-mechanical vibration of FGM sandwich beam under variable elastic foundation using differential quadrature method* Sound. Vib., **321**, 342–362, 2009.
36. A. FEREDOON, M. SGHARDOKHT SEYEDMAHALLE, A. MOHYEDDIN, *Bending analysis of thin functionally graded plates using generalized differential quadrature method*, Archive of Applied Mechanics, DOI 10.1007/s00419-010-0499-3, to appear.

Received June 28, 2011; revised version March 06, 2012.

---